Supplementary material to

Late Holocene evolution of a coupled, mud-dominated delta plain–chenier plain system, Coastal Louisiana, USA

Marc P. Hijma, Zhixiong Shen, Torbjörn E. Törnqvist, Barbara Mauz

Correspondence to: Marc P. Hijma (marc.hijma@deltares.nl)

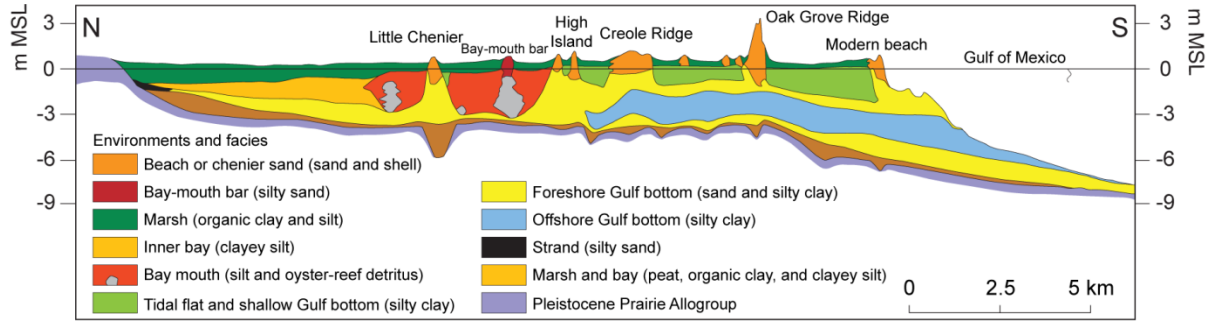

Figure S1. Regional cross section across the Chenier Plain (after Gould and McFarlan, 1959).

OSL-dating protocol

The 30-cm-long OSL samples were inspected under subdued yellow light to select the most homogenous section for dating. The outer rim (~1 cm in thickness) and two ends (1-2 cm in length) of a selected core section were cut off and used for water content and dose rate measurements, and the remaining sediments were processed following conventional procedures (Mauz et al., 2002) to extract quartz in particle-size ranges of either 4-11 μm, 75-125 μm, 125-180 μm or 180-250 μm for equivalent dose (D_e) measurement. A standard single aliquot regenerative dose (SAR) protocol with a preheating at 240 °C for 10 s and a cut-heat at 200 °C (see also Murray and Wintle, 2000; Shen et al., 2012) was applied to measure D_e at the University of Liverpool. Sand-sized quartz was measured by mounting grains onto the center 1 to 2 mm diameter area of 10 mm diameter stainless-steel disks and fine silts were mounted as a monolayer on 10 mm diameter aluminum disks by pipetting. Measured aliquots were accepted only if they show (1) a recycling ratio between 0.9 and 1.1; (2) a recuperation ratio <5%; and (3) an infrared (IR) depletion ratio between 0.9 and 1.1. The weighted mean of accepted *De* values was used for age calculation for samples measured with silt-sized quartz. The statistical procedure of Arnold et al. (2007) was used to select either a central age model (CAM) or a minimum age model (MAM, see Galbraith et al., 1999) for age calculation for samples measured with sand-sized quartz. A 10% over-dispersion was added in quadrature to the measured D_e error for all aliquots (cf. Shen et al., 2015). OSL measurements were conducted using either a Risø DA-15 B/C TL/OSL reader equipped with 27 blue light-emitting diodes (LEDs) (470Δ30 nm) or a Risø DA-15 TL/OSL reader equipped with 41 blue LEDs for optical stimulation. The luminescence emissions were detected through an optical filter (Hoya U340, 260-390 nm). The natural

radioactivity of the samples was obtained using a high-resolution, low-level gamma-spectrometer at Tulane University and converted to a natural dose rate using conversion factors of Adamiec and Aitken (1998), while the contribution of cosmic radiation was calculated using the formula of Prescott and Hutton (1994). The water content during deposition is assumed to be the same as the measured content (± 5%). OSL ages are reported in ka ± 2σ with respect to AD 2010 (Table 1).

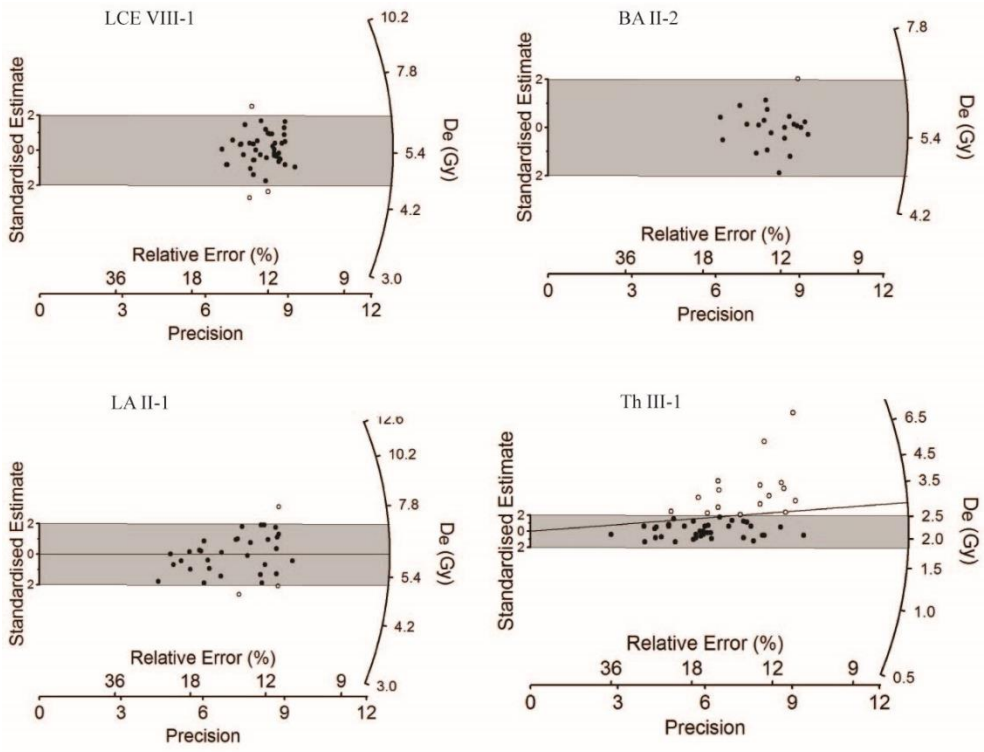

Figure S2. Radial plots of selected samples from the Chenier Plain and the Mississippi Delta Plain with each data point derived from a single aliquot. The shaded region is 2σ band of D_e derived using a central age model (CAM) for Little Chenier East (LCE) VIII-1 and Barataria (BA) II-2 and a minimum age model (MAM) for Lagan (LA) II-1 and Theriot (Th) III-1. The lines in plot for LA II-1 and Th III-1 show the CAM D_e of them. Filled dots are individual D_es fall within the shaded region.

Table S1. Corrected and calibrated radiocarbon ages from Gould and McFarlan (1959) that they labeled significant and that are located east of Calcasieu River (Fig. 1). Additional sample information was derived from Brannon et al. (1957) and McFarlan (1961). Site names follow Gould and McFarlan (1959) and McBride et al. (2007) and are partly shown in Figure 1.

Site	Lab. Code	Material dated	^{14}C age (a BP)*	Corr. ^{14}C age (a BP)†	Mean age ± 2σ‡ (cal ka before AD 2010)
Little Chenier (LC): back ridge west	O-22	*Crassostrea virginica.*	2800 ± 100	2710 ± 291	2.91 ± 0.71
Little Pecan Island			2800 ± *110*	2710 ± 291	2.91 ± 0.71
LC: back ridge west	O-12A	*Crassostrea virginica*	2750 ± 200	2660 ±335	2.83 ± 0.82
LC: front ridge west			2600 ± *110*	2510 ± 291	2.68 ± 0.72
Chenier Perdue (CP): center			2550 ± *110*	2460 ± 291	2.65 ± 0.73
LC: front ridge east	O-6	*Mulinia lateralis*	2520 ± 110	2430 ± 291	2.59 ± 0.71
CP: east			2475 ± *110*	2385 ± 291	2.51 ± 0.71
Belle Island			2400 ± *110*	2310 ± 291	2.41 ± 0.72
Mura Ridge(MR): east			2275 ± *110*	2185 ± 291	2.27 ± 0.68
MR: center			2200 ± *110*	2110 ± 291	2.16 ± 0.68
MR: west			2100 ± *110*	2010 ± 291	2.12 ± 0.67
Back Ridge			2100 ± *110*	2010 ± 291	2.12 ± 0.67
Back Chenier au Tigre			1800 ± *110*	1710 ± 291	1.76 ± 0.64
Oak Grove Rigde (OGR): back			1725 ± *110*	1635 ± 291	1.70 ± 0.67
Pelican Island Back Ridge (PIBR)	O-287	*Dinocard.* sp.	1600 ± 120	1510 ± 295	1.52 ± 0.66
PIBR	O-416	*Busycon* sp.	1600 ± 105	1510 ± 289	1.52 ± 0.66
Grand Chenier: back	O-424	*Melongela* sp.	1350 ± 105	1260 ± 289	1.30 ± 0.57
Pelican Island	O-464	*Mercenaria* sp.	1250 ± 105	1160 ± 289	1.19 ± 0.57
OGR: front	O-8	*Mulinia lateralis*	1220 ± 100	1130 ± 289	1.18 ± 0.57
Mulberry Island (MI): back			675 ± *100*	585 ± 287	0.64 ± 0.54
Mesquite Ridge (MSR)			650 ± *100*	560 ± 291	0.59 ± 0.53
MSR			450 ± *100*	360 ± 291	**0.40 ± 0.47**
Hackberry Island	O-9	*Mulinia lateralis*	520 ± 100	430 ± 291	**0.44 ± 0.50**
MSR			325 ± *100*	235 ± 291	0.33 ± 0.42
MI: front			225 ± *100*	135 ± 291	0.29 ± 0.38
MSR			100 ± *100*	10 ± 291	0.25 ± 0.34

* Errors in italics are inferred from published errors from Gould and McFarlan (1959). † To account for bulk samples, we included a 100 yr error. The dated shells are both estuarine and marine species. Based on work by Hijma et al. (2015) and Milliken et al. (2008a; 2008b) we assumed a marine reservoir effect of 400 ± 200 a. Following Hijma et al. (2015), we used a 310 ± 150 a correction for isotopic fractionation. The ages in bold were used to estimate the age of the 0.5 ± 0.3 ka paleo-shoreline (Fig. 13 and Table S2). ‡ Radiocarbon ages were calibrated with the IntCal13 curve using OxCal 4.1 (Bronk Ramsey, 2009). To facilitate comparison with the OSL ages the mean calibrated age is given relative to AD 2010.

Table S2. Major paleo-shorelines and their chronology. Note that this is not a list of all mapped paleo-shorelines in the area (for that, see McBride et al., 2007), but the ones used for calculating accumulation rates. Not all listed ridges are shown on the maps (Figs. 1 and 2).

Age ± 2σ* (ka before AD 2010)	Main Chenier	Ridges forming paleo-shoreline
2.9 ± 0.3	Little Chenier	Ridge north of High Island, Little Chenier, Little Pecan Island, Long-High-Twin-Little-Money Island, Cypress Point, Fire Island, Belle Isle trend
2.5 ± 0.2	Chenier Perdue	Back Ridge, Behind Creole Ridge, Chenier Perdue, North Island, Lambert Ridge, Pumpkin Islands
2.2 ± 0.2	Mura Ridge	Back Ridge, Center Creole Ridge, Mura Ridge, Behind Tiger Island, Back Ridge, Pumpkin Islands
1.6 ± 0.2	Pumpkin Ridge	Front Creole Ridge, Pumpkin Ridge, Tiger Island, Kochs Ridge
1.2 ± 0.1	Grand Chenier	Front Ridge, Oak Grove Ridge, Grand Chenier, Long Island, Pecan Island, Front Ridge East
0.5 ± 0.3	Mesquite Ridge	Mesquite Ridge, Mulberry Island
0	Modern shoreline	Modern shoreline

* Based on the OSL ages (Table 1). The age for the 2.5 ± 0.2 ka paleo-shoreline is based on rounding down the ages of the OSL samples. The age for the 1.6 ± 0.2 ka paleo-shoreline is based on rounding down the age of the OSL sample. The age for the 1.2 ± 0.1 paleo-shoreline is based on the rounded age of the youngest OSL sample from Grand Chenier. The age for the 0.5 ± 0.3 ka paleo-shoreline is based on Gould and McFarlan (1959, Table S1).

Table S3. Numbers used for the calculation of the temporal trends in the accumulation rates for the CP as well as the individual coastal segments (Figs. 13-15). It is assumed that the newly accumulated sediment in front of the cheniers is on average 2 m thick and has a bulk density of 1500 kg/m^3.

Paleo-shorelines				Accumulated mass in elapsed time (MT)				
age ± 2σ (ka before AD 2010)	1σ , 2σ (ka)	Elapsed time (ka)	1σ , 2σ (ka)	CP	A	B	C	D
2.90 ± 0.30	0.15, 0.30							
2.50 ± 0.20	0.10, 0.20	0.40	0.18, 0.36	255	255	148	-222	75
2.20 ± 0.20	0.10, 0.20	0.30	0.14, 0.28	367	114	176	65	11
1.60 ± 0.20	0.10, 0.20	0.55	0.14, 0.28	271	87	56	77	51
1.20 ± 0.10	0.05, 0.10	0.40	0.11, 0.22	275	330	84	-235	95
0.45 ± 0.25*	0.13, 0.25	0.75	0.14, 0.27	2184	104	803	866	411
0.03 ± 0.03	0.03, 0.06	0.42	0.13, 0.26	-62	37	-67	-49	18

*This is the unrounded estimate based on the bold numbers in Table S1.

Table S4. OSL data that were used as upper-limiting data points in Fig. 16. The error calculation was done according to the protocol described by Hijma et al. (2015). See Table 1 for the details regarding the OSL samples and ages.

Reference	Sample Name	Mean age ± 2σ (ka before AD 2010)	Limiting data elevation (m)	Total upward error (m)	Total downward error (m)
Hijma et al. (this paper)	Chenier Perdue I-1	2.58 ± 0.18	-0.32[1]	0.52[2]	0.52
Hijma et al. (this paper)	Chenier Perdue I-2	2.59 ± 0.20	-1.02	0.52	0.52
Hijma et al. (this paper)	Creole Ridge I-1	1.92 ± 0.14	-0.58	0.52	0.52
Hijma et al. (this paper)	Grand Chenier I-1	1.19 ± 0.12	0.53	0.52	0.52
Hijma et al. (this paper)	Grand Chenier II-1	1.29 ± 0.10	-1.40	0.52	0.52
Hijma et al. (this paper)	Little Chenier East IX-1	2.93 ± 0.30	-0.90	0.52	0.52
Hijma et al. (this paper)	Little Chenier West IV-1	2.94 ± 0.28	-0.54	0.52	0.52
Hijma et al. (this paper)	Pumpkin Ridge West I-1	1.66 ± 0.18	-0.25	0.51	0.51

[1]The reference water level used for calculating the limiting data elevation is the mean tide level (Hijma et al., 2015), here 0.13 m NAVD (based on Hill et al., 2011). The elevation of the midpoint of the sample of Chenier Perdue I-1 is -0.19 m NAVD resulting in limiting data elevation of -0.32 m NAVD

[2]The total error is the result of combining multiple sources of error. In this case the largest contribution comes from a conservative estimate of the error introduced by using a digital elevation model (± 0.5 m) instead of leveling equipment. Other sources come from error around the elevation of the reference water level and sampling and drilling errors.

References

Adamiec, G., Aitken, M.J., 1998. Dose-rate conversion factors: update. Ancient TL, 16 (2), 37-50.

Arnold, L.J., Bailey, R.M., Tucker, G.E., 2007. Statistical treatment of fluvial dose distributions from southern Colorado arroyo deposits. Quaternary Geochronology, 2 (1–4), 162-167. http://dx.doi.org/10.1016/j.quageo.2006.05.003.

Brannon, H.R., Simons, L.H., Perry, D., Daughtry, A.C., Jr, E.M., 1957. Humble Oil Company Radiocarbon Dates II. Science, 125 (3254), 919-923.

Galbraith, R.F., Roberts, R.G., Laslett, G.M., Yoshida, H., Olley, J.M., 1999. Optical dating of single and multiple grains of quartz from Jinmium rock shelter, northern Australia: Part I.Experimental design and statistical models. Archaeometry, 41 (2), 339-364. 10.1111/j.1475-4754.1999.tb00987.x.

Gould, H.R., McFarlan, E., 1959. Geologic history of the Chenier Plain, southwestern Louisiana. Gulf Coast Association of Geological Societies Transactions, 9, 261-270.

Hijma, M.P. et al., 2015. A protocol for a geological sea-level database. In: I. Shennan, A.J. Long, B.P. Horton (Eds.), Handbook of Sea-Level Research. Wiley Blackwell, pp. 536-553.

Hill, D.F., Griffiths, S.D., Peltier, W.R., Horton, B.P., Törnqvist, T.E., 2011. High-resolution numerical modeling of tides in the western Atlantic, Gulf of Mexico, and Caribbean Sea during the Holocene. Journal of Geophysical Research, 116, C10014-C10014.

Mauz, B. et al., 2002. The luminescence dating laboratory at the University of Bonn: equipment and procedures. Ancient TL, 20 (2), 53-61.

McBride, R.A., Taylor, M.J., Byrnes, M.R., 2007. Coastal morphodynamics and Chenier-Plain evolution in southwestern Louisiana, USA: A geomorphic model. Geomorphology, 88 (3-4), 367-422. DOI: 10.1016/j.geomorph.2006.11.013.

McFarlan, E., 1961. Radiocarbon dating of Late Quaternary deposits, south Louisiana. Geological Society of America Bulletin, 72, 129-158.

Milliken, K.T., Anderson, J.B., Rodriguez, A.B., 2008a. Record of dramatic Holocene environmental changes linked to eustasy and climate change in the Clacasieu Lake, Louisiana, USA. In: J.B. Anderson, A.B. Rodriguez (Eds.), Response of Upper Gulf Coast estuaries to Holocene climate change and sea-level rise: Geological Society of America Special Paper 443, pp. 43-63.

Milliken, K.T., Anderson, J.B., Rodriguez, A.B., 2008b. Tracking the Holocene evolution of Sabine Lake through the interplay of eustasy, antecedent topography, and sediment supply variations, Texas and Louisiana, USA. In: J.B. Anderson, A.B. Rodriguez (Eds.), Response of Upper Gulf Coast estuaries to Holocene climate change and sea-level rise: Geological Society of America Special Paper 443, pp. 65-88.

Murray, A.S., Wintle, A.G., 2000. Luminescence dating of quartz using an improved single-aliquot regenerative-dose protocol. Radiation Measurements, 32 (1), 57-73. 10.1016/s1350-4487(99)00253-x.

Prescott, J.R., Hutton, J.T., 1994. Cosmic ray contributions to dose rates for luminescence and ESR dating: Large depths and long-term time variations. Radiation Measurements, 23 (2–3), 497-500. 10.1016/1350-4487(94)90086-8.

Shen, Z. et al., 2012. Rapid and widespread response of the Lower Mississippi River to eustatic forcing during the last glacial-interglacial cycle. Geological Society of America Bulletin, 124 (5-6), 690-704. 10.1130/b30449.1.

Shen, Z. et al., 2015. Episodic overbank deposition as a dominant mechanism of floodplain and delta-plain aggradation. Geology, 43 (10), 875-878. 10.1130/g36847.1.